Light and neutron scattering studies of the OH stretching band in liquid and supercritical water

M. A. Ricci, M. Nardone, and A. Fontana[a)]
Dipartimento di Fisica ''E. Amaldi,'' Universita' degli Studi di Roma Tre, Istituto Nazionale per la Fisica della Materia, Unita' di Roma Tre. Via della Vasca Navale 84, 00146 Roma, Italy.

C. Andreani
Dipartimento di Fisica, Universita' degli Studi di Tor Vergata, Istituto Nazionale per la Fisica della Materia, Unita' di Roma Tor Vergata. Via della Ricerca Scientifica 1, 00133 Roma, Italy

W. Hahn
ISIS Facility, Rutherford Appleton Laboratory, Chilton, Didcot, Oxfordshire OX11 0QX, United Kingdom

(Received 29 July 1997; accepted 29 September 1997)

The hydrogen projected OH stretching density of states has been determined by an inelastic neutron scattering experiment in liquid and supercritical water. The results, compared with new measurements of the isotropic Raman spectra at the same state conditions, support the interpretation of the Raman spectra in terms of superposition of the allowed ν_1 band with the overtone of the ν_2 band. © *1998 American Institute of Physics.* [S0021-9606(98)50202-4]

I. INTRODUCTION

Although the spectroscopic properties of water have interested many scientists over the last decades,[1] and in spite of the large technological interest in the supercritical water properties,[2] only few studies performed in the vicinity of the critical point of water have so far appeared in the literature.[3–7] In particular the available literature on the Raman spectrum of liquid water in the region of the intramolecular O–H stretching vibration is very extensive and several review articles have been so far published.[3,8,9] Most papers however report studies performed either on pure H_2O or on H_2O–D_2O mixtures from the boiling point down to the supercooled states, while to our knowledge only a few studies[3,4,10] at temperatures higher than 100 °C have been published. On the other hand inelastic neutron scattering studies in the same energy region have become feasible since the 80s, with the advent of spallation neutron sources,[11] and only the spectra of the normal and supercooled phases of H_2O and D_2O have been studied.[12,13] In the present paper we report a study of the O–H stretching spectra of water obtained by inelastic scattering of both light and neutrons, over a wide thermodynamic range, including supercritical states, as the comparison between these two techniques can shed some light over the interpretation of the complex Raman spectral shapes.

As a matter of fact the interpretation of the peculiar lineshape of the O–H and O–D stretching bands of the Raman spectrum of water and heavy water is still a matter of contention. In both cases these bands extend over a large frequency range and display a significant component centered around their lower frequency sides, which is also quite strongly polarized.[14–16] This lower frequency component is absent from the corresponding Raman spectra of dilute solutions of HDO in either H_2O or D_2O.[4,15,17] Moreover the entire spectral lineshape shows a strong dependence on the thermodynamic state.[4,18,19] The origin of the low frequency feature of the Raman spectrum has been at various times ascribed to strong intramolecular coupling,[14] to the Fermi resonance with the bending overtone,[4,20] or to strong intermolecular coupling.[4,16,21] In particular the last point of view is based on the idea that the presence of an extended network of hydrogen bonds makes the dynamics (and hence the Raman spectrum) of water much similar to that of its amorphous solid phase. Indeed the O–H stretching spectra of amorphous solid water, as well as those of different crystalline phases, are characterized by a low frequency polarized band, which has been assigned to the symmetric vibration of neighboring molecules in phase with one another;[22,23] an interpretation which is also strongly supported by the comparison of the Raman spectrum with calculated[23] and experimental[24] vibrational density of states. In particular in the case of ice I_h the density of states calculated for the so-called reduced vibrational model[23] covers the same energy region as the observed Raman stretching band, while it underestimates the high energy side of the density of states measured in an incoherent inelastic neutron scattering experiment.[24]

II. EXPERIMENT

A. Raman scattering experiment

The sample container was an optical cell produced by the Nova Swiss, for high temperature ($T \leqslant 700$ K), medium pressures ($p \leqslant 0.1$ GPa) experiments: To avoid corrosion from high temperature water the cell body is made of stainless steel with three sapphire optical windows. Temperature control was realized, with a stability of ± 1 K, by means of a heating jacket, dissipating up to 500 W at 220 V; the sample temperature was monitored by a J-type thermocouple in thermal contact with the sample. Pressure was measured by a strain gauge and controlled, within ± 1 MPa, by a pressure

[a)]Present address: Dipartimento di Fisica, Universita' di L'Aquila, via Vetoio, 67010 Coppito (L'Aquila), Italy.

 0021-9606/98/108(2)/450/5/$15.00

TABLE I. Thermodynamic states for the light scattering experiment.

Spectrum number	T (K)	p (bar)	ρ (g/cm^3)
1	303	1	0.996
2	303	100	1.000
3	303	500	1.017
4	303	700	1.025
5	363	3	1.019
6	423	10	0.917
7	513	40	0.814
8	513	500	0.854
9	513	700	0.868
10	603	140	0.645
11	663	300	0.466

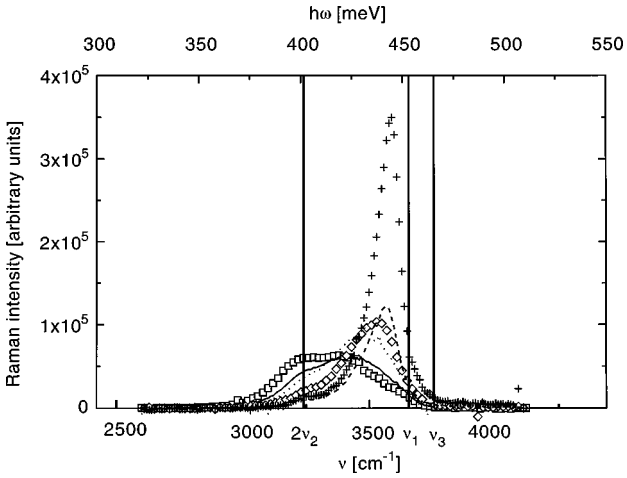

FIG. 1. The isotropic Raman spectra obtained along the coexistence curve at the thermodynamic points given in Table I, for increasing temperature and lowering density (#1: Open squares; #5: Solid line; #6: Dotted line; #7: Diamonds; #10: Dashed line; #11: Crosses). The three vertical lines indicate the position of the vibrational frequencies $2\nu_2$, ν_1 and ν_3, in the case of an isolated water molecule.

generator (Nova Swiss, type 550.0400-2). The same cell has been successfully used in a previous experiment on the Rayleigh spectrum of water.[25]

In both Raman and neutron scattering experiments samples of doubly distilled de-ionized water were degassed before filling the sample container and the sample density evaluated from the measurements of temperature and pressure, according to Ref. 26.

The Raman laser apparatus used in the experiment consists of a Spectra Physics 171 Ar-ion laser, operating at 1 W at $\lambda=514.5$ nm and of a Jobin–Yvon–Ramanor U1000 double monochromator, equipped with 1800 grooves/mm holographic gratings and a single photon counting photomultiplier. Spectra (with a resolution of 5 cm^{-1}) have been recorded in a 90° scattering configuration with VV and HV polarization.[27] The vertical V or horizontal H polarization on the sample was obtained by conveniently rotating the polarization of the incident radiation and compensating the optical anisotropy of the sapphire input window by means of a $\lambda/4$ wave plate. Similarly the V polarization of the scattered light was obtained by using a second $\lambda/4$ wave plate to compensate the optical anisotropy of the output window, before filtering through a polaroid plate. Calibration of the $\lambda/4$ wave plates was performed before pressurizing the sample. Raw spectra have been normalized to the incident intensity and corrected for dark counts and transmission of the entire apparatus, to evaluate the isotropic Raman spectra:

$$I_{\rm iso}(\tilde{\nu})=I_{VV}(\tilde{\nu})-\tfrac{4}{3}I_{HV}(\tilde{\nu}), \tag{1}$$

where $\tilde{\nu}$ represents the Raman shift measured in cm^{-1}. In the following we will discuss and compare with the neutron data only the isotropic Raman spectra. The main rational behind this choice is that the lineshapes of both polarized and depolarized Raman spectra of a dense system are likely to be distorted by the presence of interaction induced contributions and for this reason may be strongly influenced by intermolecular translational contributions, which have no counterpart in scattering by neutrons. It is known however that, among these contributions, the depolarized ones, which are by definition absent in the isotropic spectra, are the most intense.[28]

The thermodynamic states studied are reported in Table I.

Figure 1 shows the isotropic spectra obtained at a supercritical state and in the liquid phase along the coexistence curve (i.e. spectra # 1, 5, 6, 7, 10, 11 of Table I): In the same figure three vertical lines indicate the position of the first overtone of the bending mode ($2\tilde{\nu}_2$) and of the symmetric and asymmetric stretching modes respectively ($\tilde{\nu}_1$and $\tilde{\nu}_3$), for the isolated water molecule.[29] We recall that the asymmetric stretching mode is not expected to contribute to the isotropic Raman intensity, due to symmetry selection rules. Our spectra are very broad and intense, and exhibit the same strong dependence on the thermodynamic state reported in the literature.[4,10] Very good agreement with the spectra of Ratcliffe and Irish,[4] in the overlapping thermodynamic region, is found. We notice indeed that the low frequency feature of the spectrum, centered at $\tilde{\nu}=3250$ cm^{-1}, becomes less intense as the temperature increases, while the higher frequency peak moves towards the frequency of the symmetric stretching vibration of an isolated water molecule ($\tilde{\nu}_1=3656.65$ cm^{-1}) and sharpens. On the contrary increasing the density, at least in the range allowed by our experimental set-up, does not seem to affect the experimental lineshape, as demonstrated by the spectra collected along the isotherm curves at $T=303$ K and $T=513$ K (see for instance Fig. 2).

B. Neutron scattering experiment

The neutron scattering experiment has been performed using the HET chopper spectrometer installed at the ISIS pulsed neutron source (Rutherford Appleton Laboratory, UK).[30] In this spectrometer incident monochromatic neutrons are scattered by a sample located at about 12 m from the moderator and detected by ^{3}He detectors, placed at scattering angles between 3° and 140°; these are grouped into seven banks. The incident neutron energy used in the experiment was $E_i=806.38$ meV, thus allowing a resolution in energy transfer, $\hbar\omega$, better than 8 meV in the OH-stretching

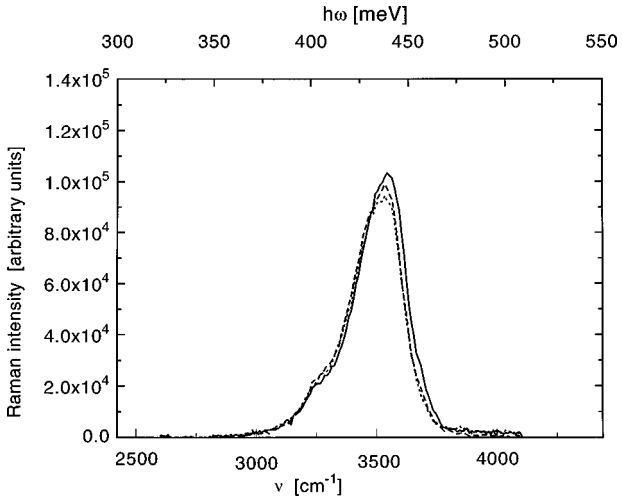

FIG. 2. The isotropic Raman spectra obtained along the isotherm at $T=513$ K, namely spectra #7 (solid line), #8 (dashed line) and #9 (dotted line) of Table I. The lineshape is almost independent on the density; the same result has been found along the isotherm at $T=303$ K.

region (namely $\hbar\omega \simeq 450$ meV), and a momentum transfer, Q, ranging between 20 and 400 nm^{-1}. The Q vs $\hbar\omega$ paths corresponding to the seven detector banks in the chosen instrument configuration are shown in Fig. 3.

Sample container was a 6.5 mm thick and 40.5 mm wide Ti–Zr slab, where an array of 6 capillaries (1.6 mm diameter) was drilled: this apparatus can withstand pressures up to 3 Kbar at a temperature of 673 K. The Ti–Zr alloy has been chosen because it does not suffer from chemical attack by high temperature water and because its contribution to the total intensity of neutrons scattered at energies higher than 300 meV is flat and negligible with respect to the scattering from water. The sample filling and pressure control was performed using a pressure rig equipped with the same pressure generator used for the Raman scattering experiment. The sample temperature was computer controlled, within ± 0.1 K, by two sensors (K-type thermocouples) and two heaters in thermal contact with the top and bottom of the sample container.

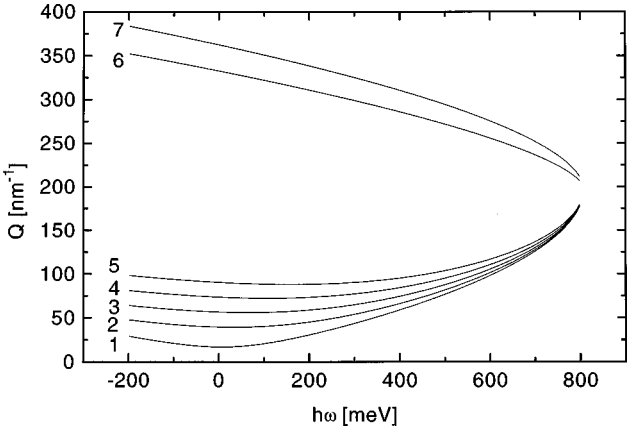

FIG. 3. The Q, $\hbar\omega$ loci corresponding to the scans performed on HET at the seven detector banks, for an incident energy $E_i = 806.38$ meV.

TABLE II. Thermodynamic states for the neutron scattering experiment.

Run number	T (K)	p (bar)	ρ (g/cm^3)
1	300	1	0.996
2	423	100	0.922
3	473	100	0.872
4	573	100	0.716
5	573	1000	0.823
6	573	2000	0.885
7	673	800	0.660

The thermodynamic states investigated have been chosen to cover roughly the same area of the T,p plane covered in the Raman scattering experiment (see Table I), and are reported in Table II.

The raw data have been corrected for contributions coming from the sample container and from multiple scattering events.[31] From the corrected data we have calculated the so-called Q-dependent density of states at each detector bank:

$$G(Q,\hbar\omega)=\frac{(\hbar\omega)^2}{Q^2}S(Q,\hbar\omega), \tag{2}$$

and then performed the extrapolation to $Q\to 0$, to evaluate the hydrogen projected density of states of water in the OH-stretching region, $g_H(\hbar\omega)$. This function for a liquid corresponds to the Fourier transform of the velocity autocorrelation function of the hydrogen atoms.[32]

The experimental results are reported in Fig. 4 for the runs # 1, 2, 3, 4, 7: Also in this figure $2\widetilde{\nu}_2$, $\widetilde{\nu}_1$ and $\widetilde{\nu}_3$, in the case of an isolated water molecule, are indicated by three vertical lines. We notice that the room temperature data are in excellent agreement with a previous experiment[12,13] performed using the HERMECS chopper spectrometer installed at the IPNS facility (Argonne National Laboratories,

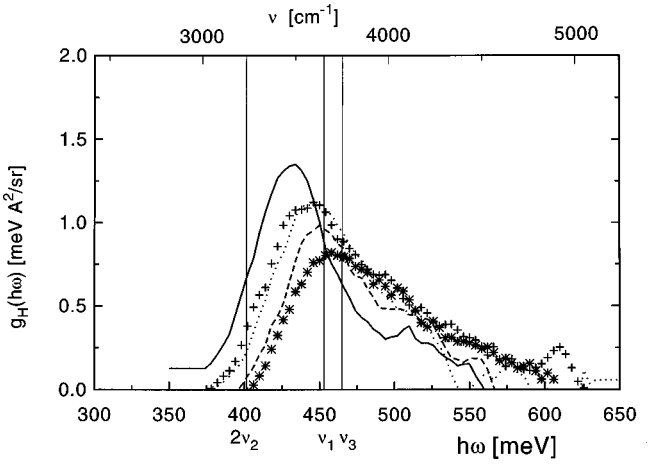

FIG. 4. The hydrogen projected density of states, $g_H(\hbar\omega)$, derived for water from neutron scattering data at ambient conditions (solid line) and for the run numbers of Table II, namely: #2 (crosses); #3 (dotted line); #4 (dashed line) and #7 (stars). The three vertical lines indicate the position of the vibrational frequencies $2\nu_2$, ν_1 and ν_3, in the case of an isolated water molecule.

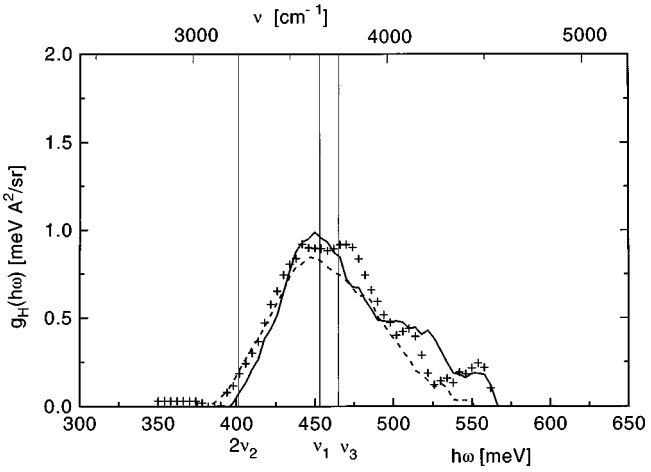

FIG. 5. The hydrogen projected density of states, $g_H(\hbar\omega)$, derived for water from neutron scattering data along the isotherm at $T = 573$ K: Namely runs #4 (solid line); #5 (crosses) and #6 (dashed line) of Table II. The three vertical lines indicate the position of the vibrational frequencies $2\nu_2$, ν_1 and ν_3, in the case of an isolated water molecule.

U.S.A.). At all state points the $g_H(\hbar\omega)$ function shows a broad main peak, followed by a second peak roughly 75 meV apart, which becomes a broad shoulder at high temperature. No clear feature corresponding to the low frequency peak of the Raman spectrum is visible. The main peak moves towards higher energies as the temperature increases; no clear dependence of the peak position on the sample density is on the contrary detected (see Fig. 5, where the data obtained along the isotherm at $T=573$ K are reported). The instrumental resolution in the investigated energy range is too poor to separate the two stretching bands, which lie only 12 meV apart in the isolated water molecule. Thus it seems reasonable to assign the main peak to the stretching vibrations, independently on their symmetry: As a matter of fact the peak position at the supercritical state goes to a limiting value which is the average of $\widetilde{\nu}_1$ and $\widetilde{\nu}_3$ (see Fig. 6). The higher energy peak may be interpreted in terms

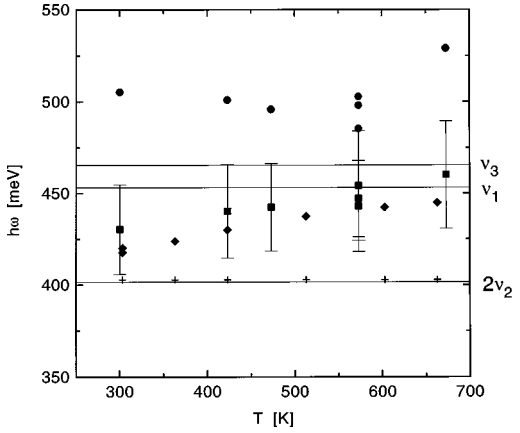

FIG. 6. Peak position of the two Gaussians fitting the isotropic Raman spectra (crosses and diamonds) and of those fitting the $g_H(\hbar\omega)$ functions derived from the neutron scattering experiment (full squares and circles). The vertical bars correspond to one standard deviation around the peak position of the lower frequency Gaussian fitting the neutron data.

of the simultaneous stretching and librational motion:[29] It is present also in the Raman spectra, although not visible in the scale of Fig. 1.

III. DISCUSSION AND CONCLUSIONS

Both the isotropic Raman spectra and the $g_H(\hbar\omega)$ function can be fitted quite satisfactorily by two Gaussians. The position of the main peaks are reported in Fig. 6 versus T. As far as the Raman spectra are concerned, we notice that for all of them the lower frequency Gaussian is centered at $\widetilde{\nu}=3250$ $\mathrm{cm}^{-1}=402.73$ meV, i. e. at a frequency only slightly higher than that of the first overtone of the free molecule bending vibration (3240 cm^{-1}). The peak of the higher frequency Gaussian on the contrary moves towards the frequency of the symmetric stretching vibration $\widetilde{\nu}_1$ as the temperature increases and is independent on the value of the density. At the same time the intensity of the lower frequency Gaussian decreases, on going towards the critical point. These findings suggest that at the lower temperatures the stretching frequency of the water molecules is strongly influenced by the motion of the neighboring molecules in the liquid: The distribution of these frequencies is then shifted to lower values (i.e. towards the first overtone of the bending vibration), due to inter- and intra- molecular couplings, and the Raman intensity of the overtone vibration is enhanced by the Fermi resonance.

The neutron scattering data, as already stated, do not exhibit any structure on the low frequency side of the main peak: The position of this peak moves with the temperature towards higher frequencies, following the behavior of the higher frequency Gaussian of the Raman spectra, although neutron data lie on a curve systematically higher than that followed by the Raman data and reach a frequency which is intermediate between $\widetilde{\nu}_1$ and $\widetilde{\nu}_3$ at the supercritical states. As already stated this is consistent with the fact that we are not resolving the two stretching modes in the present instrumental configuration. In Fig. 6 we have represented by vertical bars the interval around the peak position, corresponding to one standard deviation of the Gaussian, to demonstrate that if a spectral feature at $2\widetilde{\nu}_2$ were present in the neutron data, this should be resolved from the main peak. The higher frequency Gaussian used to fit the neutron scattering data does not show any clear behavior with the thermodynamic state: It is well resolved at the lower temperature states and then merges into a broad high energy tail of the main peak. We recall that a spectral feature centered at roughly the same frequency, although with much lower intensity, is visible also in the Raman spectra and is usually interpreted in terms of combined stretching and librational motions. On the other hand also Ref. 24 shows similar differences between Raman and neutron scattering data in the solid phase of water and it has to be mentioned that this high energy tail of the neutron data may be biased by a poor correction of the multiple scattering contribution.

Inspection of Fig. 6 supports the interpretation of the Raman isotropic spectra given at the beginning of this section: The higher frequency feature of the spectrum does in-

deed move with the temperature as the main feature of the corresponding density of states does. Moreover, contrarily to what found in the case of various solid forms of water, we do not have, at any temperature, a complete coverage between Raman and neutron spectra at the lower frequencies, thus invalidating a possible interpretation of the low frequency feature of the isotropic spectrum in terms of the density of states corresponding to in phase vibrational motions of cluster of molecules. We notice also that such interpretation could not however be expected to hold at temperatures close to the critical one, where the microscopic structure of water has suffered strong distortions with respect to that of ambient and supercooled water.[33] On the other hand it does not seem necessary to invoke two different mechanisms of modulation of the polarizability derivative at low and high temperatures, since the spectral shape modifications are continuous.

ACKNOWLEDGMENTS

The authors acknowledge the skilled technical support of Mr. A. P. Russo (Universita' degli Studi di Roma Tre), Mr. I. F. Bailey, Mr. J. W. Dreyer and Mr. J. A. Bones (Rutherford Appleton Laboratory). This work has been partially supported by the Italian Consiglio Nazionale delle Ricerche.

[1] *Water: A Comprehensive Treatise*, Vols. 1–7, edited by F. Franks (Plenum, New York, 1970).
[2] C. A. Eckert, B. L. FKnutson, and P. G. Debenedetti, Nature (London) **383**, 313 (1996).
[3] E. U. Franck, in *Structure of Water and Aqueous Solutions*, edited by A. P. Luck (Verlag Chemie, Weinheim, West Germany, 1974), p. 49.
[4] C. I. Ratcliffe and D. E. Irish, J. Phys. Chem. **86**, 4897 (1982).
[5] A. Fontana, M. Nardone, and M. A. Ricci, J. Chem. Phys. **102**, 6975 (1995).
[6] E. U. Franck and K. Roth, Discuss. Faraday Soc. **43**, 108 (1967).
[7] G. V. Bodarenko, and Yu. E. Gorbatyi, Dokl. Akad. Nauk SSSR **210**, 132 (1974).
[8] J. R. Scherer, in *Advances in Infrared and Raman Spectroscopy*, edited by R. J. H. Clark and R. E. Hester (Heiden, London, 1978), Vol. 5, p. 149.
[9] M. A. Ricci, in *Hydrogen Bond Networks*, edited by M. C. Bellissent-Funel and J. C. Dore (Kluwer, Netherland, 1994), p. 205.
[10] D. A. Masten, B. R. Foy, D. M. Harradine, and R. B. Dyer, J. Phys. Chem. **97**, 8557 (1993).
[11] C. G. Windsor, *Pulsed Neutron Scattering* (Taylor & Francis, London, 1981).
[12] S. H. Chen, K. Toukan, C. K. Loong, D. L. Price, and J. Teixeira, Phys. Rev. Lett. **53**, 1360 (1984).
[13] K. Toukan, M. A. Ricci, S. H. Chen, C. K. Loong, D. L. Price, and J. Teixeira, Phys. Rev. A **37**, 2580 (1988).
[14] J. R. Scherer, M. K. Go, and S. Kint, J. Phys. Chem. **78**, 1304 (1974).
[15] J. Wiafe-Akenten and R. Bansil, J. Chem. Phys. **78**, 7132 (1983).
[16] D. E. Hare and C. M. Sorensen, J. Chem. Phys. **93**, 25 (1990); Chem. Phys. Lett. **190**, 605 (1992).
[17] K. Cunningham and P. A. Lyons, J. Chem. Phys. **59**, 2132 (1973).
[18] G. E. Walrafen, in *Water: A Comprehensive Treatise*, Vols. 1–7 (Plenum, New York, 1970); G. E. Walrafen, M. S. Hokmabadi, and W. H. Yang, J. Chem. Phys. **85**, 6964 (1986).
[19] G. D'Arrigo, G. Maisano, F. Mallamace, P. Migliardo, and F. Wanderlingh, J. Chem. Phys. **75**, 4264 (1981).
[20] Yu. Ya. Efimov, J. Mol. Struct. **141**, 419 (1986); Yu. Ya. Efimov and Yu. I. Naberukhin, Faraday Discuss. Chem. Soc. **85**, 117 (1988).
[21] J. L. Green, A. R. Lacey, and M. G. Sceats, Chem. Phys. Lett. **130**, 67 (1986); J. Chem. Phys. **91**, 1684 (1987).
[22] P. T. T. Wong and E. Whalley, J. Chem. Phys. **62**, 2418 (1975); E. Whalley, Can. J. Chem. **55**, 3429 (1977).
[23] T. C. Sivakumar, S. A. Rice, and M. G. Sceats, J. Chem. Phys. **69**, 3468 (1978); R. Mc Graw, W. G. Madden, M. B. Bergen, S. A. Rice, and M. G. Sceats, *ibid.* **69**, 3483 (1978).
[24] C. Andreani, P. Bosi, F. Sacchetti, and C. K. Loong, J. Chem. Phys. **83**, 750 (1985).
[25] A. Fontana, M. Nardone, and M. A. Ricci, J. Chem. Phys. **102**, 6975 (1995).
[26] R. Hilbert, K. Todheide, and E. U. Franck, Ber. Bunsenges. Phys. Chem. **85**, 636 (1981); Landolt-Bornstein, *Zahlenwerte und Funktionen aus Phisik, Chemie, Astronomie, Geophisik und Technik* (Springer, Berlin, 1967), Vol. IV-4a.
[27] The polarization directions are conventionally reported following B. H. Berne and R. Pecora, in *Dynamic Light Scattering* (Wiley, New York, 1976).
[28] *Phenomena Induced by Intermolecular Interactions*, edited by G. Birnbaum, NATO ASI Series, Series B: Physics (Plenum, New York, 1985), Vol. 127.
[29] D. Eisemberg, and W. Kauzmann, *The Structure and Properties of Water* (Oxford at the Clarendon Press, 1969).
[30] R. S. Eccleston and R. Osborn, Report RAL-94-117 (1994).
[31] V. F. Sears, Adv. Phys. **24**, 1 (1975); C Andreani, V. Merlo, M. A. Ricci, and D. Lepoire, Nucl. Instrum. Methods Phys. Res. B **61**, 123 (1991).
[32] S. H. Chen and S. Yip, Phys. Today **29**, 32 (1976).
[33] P. Postorino, R. H. Tromp, M. A. Ricci, A. K. Soper, and G. W. Neilson, Nature (London) **366**, 668 (1993); A. K. Soper, F. Bruni, M. A. Ricci, J. Chem. Phys. **106**, 247 (1997).